JOURNAL OF NANO- AND ELECTRONIC PHYSICS
Vol. **16** No 5, 05007(5pp) (2024)

ЖУРНАЛ НАНО- ТА ЕЛЕКТРОННОЇ ФІЗИКИ
Том **16** № 5, 05007(5cc) (2024)

OPEN ACCESS

REGULAR ARTICLE

Development of a Compact Patch Antenna with Ladder-Slot Configuration for Wearable Applications Towards WBAN / ISM Band

A.S. Burra*, B. Roy†

SENSE, VIT – AP University, Amaravati, Andhra Pradesh, 522237 India

(Received 12 June 2024; revised manuscript received 19 October 2024; published online 30 October 2024)

This paper introduces a compact patch antenna with ladder-slot configuration designed for wearable applications. The antenna achieves miniaturization through the incorporation of partial ground and slots on the patch. Operating within the frequency range of 1.5 GHz (lower limit) to 3.8 GHz (upper limit), it covers the wireless body area network (WBAN) and the industrial, scientific, and medical (ISM) frequency bands. It's designed on an epoxy FR-4 substrate with a dielectric constant (ε_r) of 4.4 and a thickness of 1.6 mm, the antenna resonates specifically at 2.4 GHz. This resonating frequency boasts an impressive impedance bandwidth of 2.3 GHz (equivalent to 86.80%), while maintaining a compact size of $0.42\lambda \times 0.40\lambda$ mm². Notably, the antenna exhibits remarkable attributes such as high directivity, favorable cross-polarization levels, and efficiency at its resonating frequency. These features position it as a strong candidate for employment in both WBAN and ISM band Internet of Things (IoT) applications. This can be used in Mobile phones, Bluetooth devices, Wi-Fi Devices, wireless communication and Wearable applications. The antenna's small size, cost-effectiveness, omnidirectional radiation pattern, and reliable far-field characteristics make it a promising choice for wearable applications.

Keywords: WBAN, Partial ground, Wearable patch antenna, ISM band, 2.4 GHz, Ladder-slot.

DOI: 10.21272/jnep.16(5).05007 PACS numbers: 73.61.Jc, 71.20.Mq, 88.40.jj, 88.40.hj

1. INTRODUCTION

Over the past few years, the proliferation of wireless networks and diverse electronic devices has spurred the widespread adoption of wireless body area networks (WBANs). These networks find application across a spectrum of scenarios, facilitating the integration of wearable antenna technology for data transmission and reception [1]. The utility of wearable antennas spans various domains such as GPS navigation, military operations, athletic performance tracking, healthcare services, consumer electronics, and smart watches [2].

Particularly in healthcare, wireless medical sensor systems have become pivotal for continuous health monitoring, offering the ability to access physiological data remotely. The placement of sensors with-in the human body equips medical professionals with real-time health insights, transcending geographical boundaries. By ensuring continuous monitoring in typical physiological conditions, WBANs lay the groundwork for an advanced healthcare ecosystem capable of proactive crisis management and early detection of chronic illnesses. This encompasses wireless computation and monitoring of electro cardio grams, respiration rates, electroencephalograms (EEG), body temperatures, electromyograms (EMG), and blood pressure through WBAN-installed sensors [3-5].

To realize the envisioned capabilities, it is imperative to devise compact, inconspicuous, comfortable, and lightweight wearable antenna solutions. The literature extensively documents efforts towards wearable antennas tailored for WBANs and applications within the industrial, scientific, and medical (ISM) frequency bands. Achieving efficient device integration necessitates advancements in areas such as miniaturization and biocompatibility. Strategies involving slot insertion and the introduction of defective ground structures have yielded various miniaturization techniques.

Additionally, optimization of ground connections with radiating rectangular patches has emerged as an avenue for enhancing bandwidth and radiation patterns [6-8]. Capitalizing on the synergy between the Internet of Things (IoT) and wearable devices offers enhanced automation and reduced hardware and labor costs.

An essential facet in the development of microstrip patch antennas for wearable's involves the realization of a radiating patch using flexible conductive materials, complemented by an adaptable ground plane and substrate

* Correspondence e-mail: swamy.22phd7046@vitap.ac.in
† bappadittya.roy@vitap.ac.in

Cite this article as: A.S. Burra et al., *J. Nano- Electron. Phys.* 16 No 5, 05007 (2024) https://doi.org/10.21272/jnep.16(5).05007

material. In light of this backdrop, the present study presents a novel approach: a ladder-shaped slotted patch antenna design, engineered to resonate at 2.4 GHz—a frequency of significant relevance for WBAN [9] and ISM band applications. The integration of slots and a partial ground in the antenna's architecture contributes to an expanded bandwidth, yielding an impressive impedance bandwidth (IBW) of 86.80%. The subsequent sections delve into the specifics of the antenna's geometry (Section 2), elucidate simulation results (Section 3), and culminate in the conclusion (Section 4). The synthesis of these design elements contributes to a promising wearable microstrip antenna that holds potential for advancing WBAN and ISM band functionalities.

2. ANTENNA CONFIGURATION

The envisioned antenna design comprises three layers, wherein an FR-4 substrate boasting a dielectric constant of 4.4 and a loss tangent (tan δ) of 0.025 acts as a separator between two parallel copper metal plates, as depicted in Fig. 1. A novel adaptation involves the integration of a modified rectangular patch embellished with a ladder-shaped slot etched onto the patch's surface, coupled with a strategically positioned partial ground. This composite architecture is strategically engineered to facilitate the attainment of desired resonance frequencies. Noteworthy is the precise placement of slots on the patch, a crucial facet enhancing the simulation's overall performance. Gap slot (L5, W5) is maintained to achieve better characteristics. All slots and truncated patch modifications as shown in Fig. 1 (a-e).

The judicious inclusion of a partial ground plane serves a twofold purpose: firstly, it reduces unwanted back lobe radiations by reducing the amount of surface waves that are diffraction from the antenna's edge to the ground plane; secondly, it introduces supplementary reactance at the feeding point, thereby contributing to the realization of an ultra-wideband response. To further extend the antenna's bandwidth and achieve wideband resonance within the 2.4 GHz spectrum (ranging from 1.5 GHz to 3.8 GHz), strategic modifications are applied to both the ground plane and the patch antenna. The detailed optimized antenna measurements are given in Table.1. These modifications induce perturbations in the electric field's trajectory, ultimately leading to the desired broadband resonance effect.

Excitation of the proposed antenna is carried out through a 50Ω microstrip feed line. The design and optimization process leverages the capabilities of a high-frequency structure simulator (HFSS). Prior to embarking on the antenna design within an electromagnetic (EM) simulator, a set of fundamental design parameters is determined through pertinent equations, laying the groundwork for the proposed antenna's development.

Width of the Patch

$$W = \frac{c}{2 f_r}\sqrt{\frac{2}{\epsilon_r+1}}$$

Where c – Speed of the light, f_r – Resonant frequency, ε_r – Dielectric constant of the substrate.

In the process of microstrip antenna design, a critical consideration is the effective refractive index. As radiation emanates from the patch and traverses towards the ground, a portion travels through the surrounding air while another portion follows a path through the substrates — a phenomenon referred to as fringing. To accurately capture these interactions, it becomes imperative to ascertain the effective dielectric constant, as the substrates and air exhibit disparate dielectric characteristics. This pivotal parameter, denoted as the effective dielectric constant ($\in_{reff}$), is quantified utilizing the subsequent equation [5].

$$\epsilon_{reff} = \frac{\epsilon_r+1}{2} + \frac{\epsilon_r-1}{2}\left[1 + 12\,\frac{h}{w}\right]^{-\frac{1}{2}}$$

The following formulas must be used to determine the patch's length:

Length of the Patch, $L = L_{eff} - 2\Delta L$

Where

$$\Delta L = 0.412 \cdot h \cdot \frac{(\epsilon_{reff}+0.3)\,(\frac{w}{h}+0.264)}{(\epsilon_{reff}-0.258)\,(\frac{w}{h}+0.8)}$$

Effective length

$$L_{eff} = \frac{c}{2\, f_r \sqrt{\epsilon_{r\,eff}}}$$

Now, calculate the feed measurements using below equations, Feed length is $\lambda_g/4$. Where

$$\lambda_g = \frac{\lambda}{\sqrt{\epsilon_{reff}}}$$

2.1 Specific Absorption Rate (SAR)

The Specific Absorption Rate is a measurement of how much RF energy is absorbed by human tissue. The evaluation of Specific Absorption Rate (SAR) assumes paramount importance, given the antenna's intended wearable usage, in order to mitigate potential health risks. In the context of functioning as a biomedical antenna, an in-depth analysis is conducted utilizing a specialized three-layer human phantom model. This model serves a dual purpose: firstly, it investigates the nuanced alterations in the antenna's behavior when deployed in on-body biomedical applications, and secondly, it quantifies the potential impact of the antenna on the human body. Central to the construction of this phantom model are the electromagnetic properties of diverse human tissues, encompassing their permittivity and conductivity profiles.

The dimensions pertaining to the constituent human biological tissues, which constitute the foundation of the human phantom, are meticulously outlined in Table 2. This tabulation encapsulates key attributes including density, permittivity, conductivity, and loss tangent for distinct bodily organs. The tri-layer human phantom model comprises muscle, fat, and skin as its constituents.

Notably, the antenna under consideration yields a Specific Absorption Rate (SAR) value of 0.246 W/Kg.

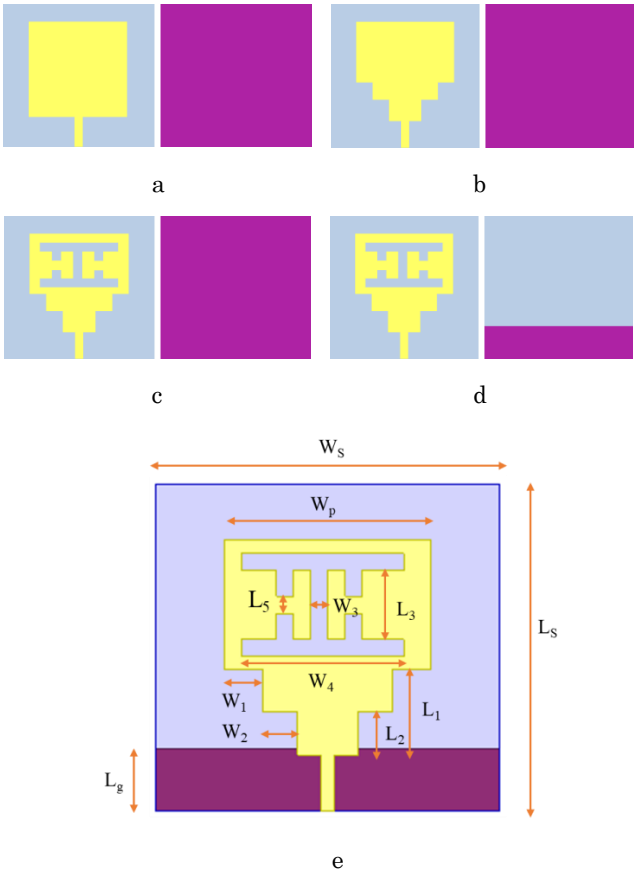

Fig. 1 – (a-d) Design evolution of the proposed antenna, (e) Dimensions of the proposed design

Table 1 – Optimized dimensions

Parameter	L_p	W_p	L_g	W_g	L_s	h
Dimension (mm)	25	24	7.2	40	38	1.6
Parameter	W_s	L_1	W_1	L_2	W_2	L_3
Dimension (mm)	40	10	4.5	5	4	8
Parameter	W_3	L_4	W_4	L_5	W_5	
Dimension (mm)	2	2	18.8	2	2	

Table 2 – Tissues properties of Human Tissue

Human Tissue	**Density Kg/m³**	**Permittivity, ϵ_r**	**Conductivity, s/m**	**Loss tangent, δ**
Skin	1100	31.29	5.0138	0.2835
Fat	1100	5.28	0.1	0.19382
Muscle	1060	52.79	1.705	0.24191

3. SIMULATED RESULTS

The section elaborates on the outcomes of the simulation performed for the suggested antenna configuration. A comprehensive simulation was undertaken, utilizing HFSS software, to fine-tune the antenna dimensions for optimal performance. The return loss, indicative of energy loss in a signal due to transmission line perturbations, was meticulously analyzed.

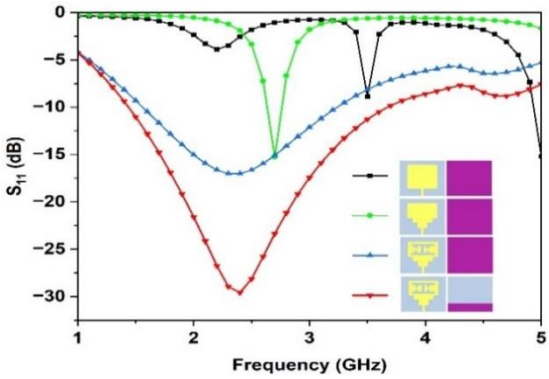

Fig. 2 – Reflection Coefficient (S_{11}) Curve at different design steps

The graphical representation illustrating the relationship between antenna bandwidth, return loss (S_{11}), and frequency shown in Fig. 2 facilitates the identification of resonating frequency with different modification levels of patch from (a) to (d) to achieve proposed structure. Consequently, the frequency exhibiting minimal return loss is deemed the resonating frequency 2.4 GHz. In this context, the antenna's bandwidth is conclusively established to be 2.3 GHz, spanning from 1.5 GHz to 3.8 GHz.

The Voltage Standing Wave Ratio (VSWR) relative to frequency for the proposed antenna geometry. The transmission line achieves successful matching with the antenna, supported by a VSWR of 1.0687 at 2.4 GHz, remaining below 2 across the entirety of the operational frequency spectrum. Within the complete operational range, a compelling convergence is observed. The real component (Resistance) approaches proximity to 50Ω, while the imaginary component (Reactance) converges towards 0Ω at resonant frequencies. This substantiates the entire impedance nearing the desired 50Ω benchmark, signifying successful impedance matching.

At the resonant frequency of 2.4 GHz, Fig. 3 illustrates the distribution of surface currents within the proposed configuration. A noteworthy observation emerges from this depiction, indicating active participation in radiation by both the ground plane and patch.

In Fig. 4, the plot illustrates the variation in gain and efficiency across different frequencies. Notably, at higher frequencies, a marginal reduction in efficiency is observed, attributed to the combined impact of Ohmic and radiation losses. At its zenith, the antenna attains a peak gain of 0.6 dBi precisely at 2.4 GHz, accompanied by an impressive peak radiation efficiency of 96.59%.

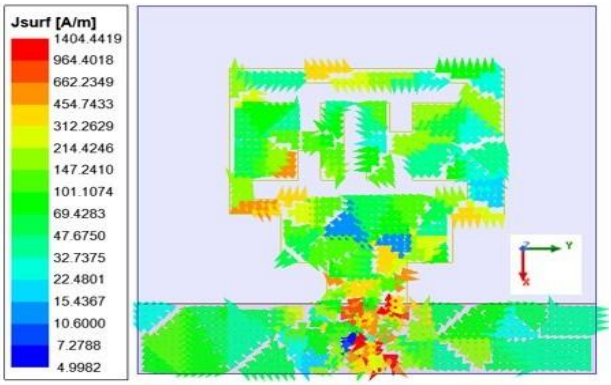

Fig. 3 – Surface current distribution at 2.4 GHz

The concept of antenna gain serves as a quantitative descriptor of an antenna's power transmission capacity in relation to an isotropic antenna. This parameter encapsulates an antenna's ability to both transmit and receive signals within specific directions, as defined by established standards. The gain plot conspicuously demonstrates a linear growth trajectory across the antenna's operational frequency spectrum, mirroring the fundamental principles governing antenna behavior, where gain invariably escalates with escalating frequencies.

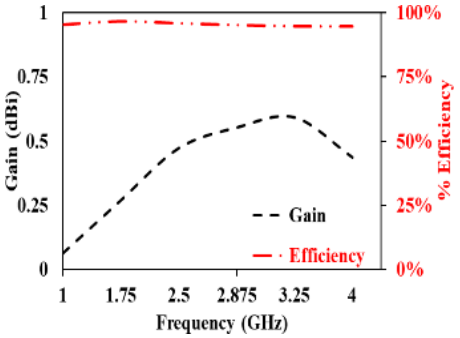

Fig. 4 – Gain and Radiation Efficiency Vs Frequency plot

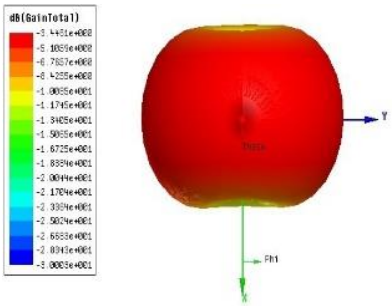

Fig. 5 – 3D Gain of the antenna

Within the antenna design, the antenna's inherent propensity to exhibit varying radio wave strengths in distinct directions is encapsulated by the term "radiation pattern". A three-dimensional rendition of this phenomenon, referred to as the 3D Radiation Pattern, graphically illustrates how an antenna disseminates electromagnetic energy into the surrounding space. This visual representation is vividly portrayed in Fig. 5, offering an insightful depiction of the spatial distribution of electric transmission by the antenna.

Fig. 6 illustrates the two-dimensional far-field radiation pattern simulated at the resonant frequency of 2.4 GHz, showcasing its maximum gain. Notably, the design showcases consistent and favorable radiation patterns within both the φ = 00 plane (E-plane), exhibiting an eight-shaped pattern, and the 900 plane (H-plane), taking on a circular pattern. This radiation pattern configuration aligns with the coveted attributes of an omnidirectional antenna's Radiation Pattern (RP), contributing to a holistic coverage. The implications of this radiation pattern are reflected in the antenna's gain, which is intentionally lower in the main lobe direction, in accordance with the inherent characteristics of omnidirectional antennas.

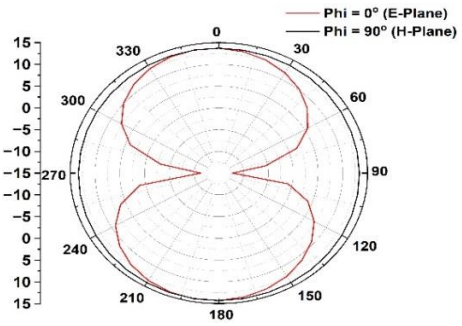

Fig. 6 – 2-D E-plane and H-plane RP of the proposed antenna at 2.4 GHz

The comprehensive evaluation of the antenna's performance extends to its interaction within free space conditions, as well as its interaction with the phantom muscle. This assessment underscores the antenna's overall harmonious performance across varying scenarios.

3.1 Parametric Analysis

Parametric analysis is completed with gap slots of the ladder patch antenna. L5 of the slot varied from 0 to 2 mm with a step of 0.5 then it given good reflection coefficient, variation in resonant frequency and upper cut off frequency varied from low to high. This analysis as shown in Fig. 7.

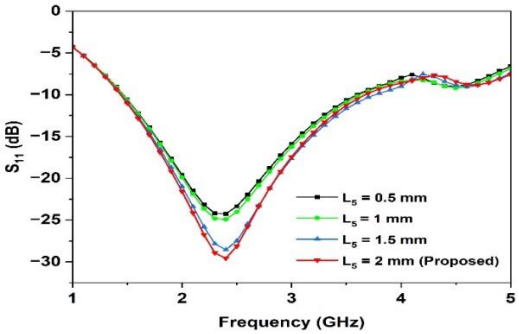

Fig. 7 – Parametric analysis of the proposed Antenna

3.2 Fabricated Antenna Results

Simulated and measured reflection coefficient of the fabricated prototype of the proposed Compact antenna comparison as shown in Fig. 8. Measured radiating frequency is equal to the simulated and given same characteristics of the proposed antenna.

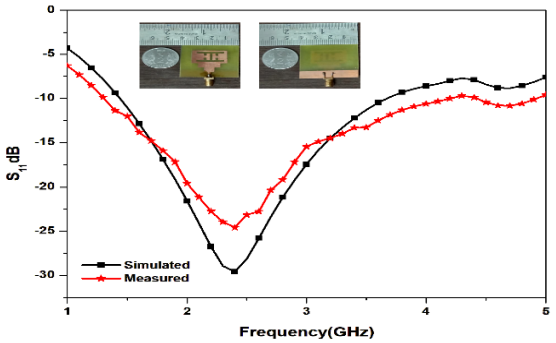

Fig. 8 – Simulated and measured reflection coefficient of the proposed Antenna

4. CONCLUSION

In this paper, a compact patch antenna with ladder slot configuration for wearable applications towards WBAN and ISM band applications has been developed, analyzed and simulated. The antenna, compact at $40 \times 38 \times 1.6$ mm^3, exhibits an impressive 2.3 GHz bandwidth, outperforming existing counterparts. At 2.4 GHz, it demonstrates a return loss of – 29.18 dB and a VSWR of 1.0687, ensuring effective health monitoring capabilities. Then importantly, the antenna's Specific Absorption Rate (SAR) value is 0.246 W/Kg, well below safety thresholds, affirming its suitability for human use without radiation risks. The antenna's small size, cost-effectiveness, omnidirectional radiation pattern, and reliable far-field characteristics make it a promising choice for wearable applications towards WBAN/ISM band.

REFERENCES

1. A. Arif, M. Zubair, M. Ali, M.U. Khan, M.Q. Mehmood, *IEEE Anten. Wireless Propag. Lett.* **18** No 5, 981 (2019).
2. F. Khajeh-Khalili, Y. Khosravi, Taylor, *Francis The Journal of Textile Institute* **112**, 1266 (2021).
3. A. Sabban, *Electronics* **11** No 3, 427 (2022).
4. K. Harvinder, P. Chawla, *Int. J. Electron.* **110** No 6, 986 (2023).
5. B. Roy, A.K. Bhatterchya, S.K. Choudhury, *International Conference on Microwave and Photonics* (ICMAP), 1 (2013).
6. S. Hussain, S. Hafeez, S.Ali Memon, N. Pirzada, *International Journal of Advanced Computer Science and Applications (IJACSA)* **9** No 9 (2018).
7. Z. Yu, R. Niu, G. Zhang, R. Sun, Z. Lin, Y. Li, X. Ran, *IEEE Access* **11**, 87930 (2023).
8. J. Jaiverdhan, M.M. Sharma, R.P. Yadav, R. Dhara, *Progr. Electromagn. Res. M* **94**, 105 (2020).
9. W. Saadat, S.A. Raurale, G.A. Conway, J. McAllister, *IEEE Trans. Anten. Propag.* **70** No 1, 17 (2022).

Розробка компактної патч-антени з конфігурацією сходів і слотів для носимих додатків у діапазоні WBAN / ISM

A.S. Burra, B. Roy

SENSE, VIT – AP University, Amaravati, Andhra Pradesh, 522237 India

У цій статті представлено компактну патч-антену з конфігурацією драбинчастого слота, призначену для застосування в носимих пристроях. Мініатюрність антени досягається за рахунок часткового заземлення та прорізів на накладці. Працюючи в діапазоні частот від 1,5 ГГц (нижня межа) до 3,8 ГГц (верхня межа), він охоплює бездротову мережу на тілі (WBAN) і промислові, наукові та медичні (ISM) діапазони частот. Вона розроблена на основі епоксидної смоли FR-4 з діелектричною проникністю (ε_r) 4,4 і товщиною 1,6 мм, антена резонує саме на 2,4 ГГц. Ця резонансна частота може похвалитися вражаючою смугою пропускання імпедансу 2,3 ГГц (еквівалентно 86,80 %), зберігаючи при цьому компактний розмір $0{,}42\lambda \times 0{,}40\lambda$ мм^2. Примітно, що антена демонструє чудові властивості, такі як висока спрямованість, сприятливі рівні крос-поляризації та ефективність на її резонансній частоті. Ці особливості позиціонують його як сильного кандидата на роботу в додатках Інтернету речей (IoT) як у WBAN, так і в діапазоні ISM. Це можна використовувати в мобільних телефонах, пристроях Bluetooth, пристроях Wi-Fi, бездротовому зв'язку та програмах, які можна носити. Невеликий розмір антени, економічна ефективність, всеспрямована діаграма спрямованості та надійні характеристики дальнього поля роблять її перспективним вибором для носимих пристроїв.

Ключові слова: WBAN, Часткове заземлення, Носима патч-антена, Діапазон ISM, 2,4 ГГц.